Tracking Operations During the Helios 2 Launch Phase

L. E. Bright
Network Operations Section

The prelaunch planning for the DSN's participation in the launch of the Helios 2 spacecraft is reviewed from the point of view of the tracking function. The actual events of the initial acquisition are discussed and analyzed in relation to prelaunch plans. In addition, an analysis of the effects of the Helios 2 spacecraft's spin on doppler data is provided.

I. Introduction

The relative infrequency of launches of deep space probes and the uniqueness of the demands they place on the DSN for an initial acquisition make it essential that the experience gained in each launch phase be carefully preserved and documented so that it may be applied to best effect in future launches. With this in mind, the present report summarizes the DSN's planning for and operations during the Helios 2 launch phase from the viewpoint of the tracking function. (The Helios-2 liftoff occurred at the open window launch time of 05:34:00.8 GMT on January 15, 1976. All GMT event times in this report unless otherwise stated are on January 15, 1976.)

Section II covers the planning activities for the launch and initial acquisition while Section III discusses and analyzes the actual launch phase operations at the Network Operations Control Center (NOCC) and at the Australian Deep Space Stations, DSSs 42 and 44, the prime and backup initial acquisition stations, respectively. A summary and conclusions are offered in Section IV.

II. Prelaunch Planning

Planning for the initial acquisition of a new spacecraft begins many months before the actual launch. In the case of Helios 2, of course, most of the planning for and all of the experience gained in the Helios 1 launch were directly applicable. The Viking launches between the two Helios launches also provided valuable experience to personnel at the DSSs and at JPL.

For the tracking function, the "on paper" phase of preparation for launch culminated with an Initial Acquisition Plan for Helios 2 issued by the Tracking Element of the Network Operations Analysis Group (NOAG). Prepared by the present author with the generous assistance of other members of the NOAG and DSN Operations, the plan defined a baseline strategy for the initial acquisition to which minor refinements were made as a result of operational testing and other preparatory activities. That plan is summarized in the following paragraphs.

A. Features Peculiar to the Helios Spacecraft

Several unique features of the Helios spacecraft had a significant impact on initial acquisition planning. The first of these was the so-called "silent spacecraft mode," a spacecraft configuration in which the transmitter has been automatically switched off due to a momentary drop in spacecraft power. To reactivate the transmitter, it is necessary to acquire the uplink "in the blind" and subsequently command the transmitter back on. Obviously, this adds a new element of uncertainty into the initial acquisition process: does a failure to detect the spacecraft signal result from erroneous ground receiver settings or from mispointing of the station's antenna (frequency and angle uncertainties are always high during a launch phase), or is the spacecraft simply not transmitting a signal?

Another special consideration was the "interference zone." The changing aspect angle of the ground station as viewed by the spacecraft carries the radio line-of-sight through a region where the dual elements of the spacecraft low-gain antenna interfere destructively. This, combined with the fact that the spacecraft is spinning rapidly while transmitting through an antenna that is offset from the spin axis, produces a very complex amplitude and frequency modulation of the downlink signal. Consequently, the possibility of losing lock on the downlink during this period had to be allowed for in the acquisition procedures.

A final point that had to be considered was that the downlink signal is not automatically switched to coherent mode when the uplink is acquired. The coherent mode is brought about only by ground command. Consequently, there is no change in downlink frequency (with the resulting receiver-out-of-lock condition) that normally accompanies a successful uplink acquisition. Moreover, station and Network Operations Control Team (NOCT) personnel must be prepared for a change in frequency when the downlink *is* switched to coherent.

B. Trajectory Considerations

The tracking parameter rates seen by DSS 42 in the Helios launch phase trajectories could only be considered extreme when compared to the rates seen in previous launch passes. For example, during the launch opportunity period January 15–February 7, 1976, a typical Helios 2 two-way doppler (D2) rate might reach 500 Hz/s, which would be among the highest D2 rates seen in any launch phase and nearly twice the highest rate observed during the Helios 1 launch. Angle rates would also be extreme. (These trajectory features may be seen in Figs. 1 and 2, which depict the DSS 42 pass in terms of a stereographic projection of apparent spacecraft motion and nominal best-lock frequency curve, respectively.) Other general observations of interest were:

(1) The Helios 2 trajectory rates would be highest at the open window of any given launch date, and would diminish monotonically as the launch time progressed into the (daily) window.

(2) Trajectory rates would increase from day to day throughout the launch opportunity, reaching their extreme values the last day of the opportunity.

(3) The launch pass at DSS 42 would have a duration of from 5½ to 7 hours, with the retrograde point occurring at about 1½ hours after rise.

For the actual Helios 2 launch date and time the resulting tracking rates were typical of the range of possible values through the entire launch opportunity. Actual peak values were:

$$\text{Hour angle rate} = 0.157 \text{ deg/s}$$

$$\text{D2 rate} = 549 \text{ Hz/s}$$

This D2 rate does not include spin modulation effects which can, under the worst conditions (see Section III-G), more than double the instantaneous rate. Still a D2 rate of 1200 Hz/s is quite tolerable under high signal level conditions, giving a phase-locked-loop phase error of only about 6 degrees. The angle rates were also well within tracking capabilities.

Based on Helios 1 experience, the following 3σ uncertainties in tracking observables were assumed for the Helios 2 launch pass:

$$\Delta\text{Hour Angle} \approx 1.2 \text{ deg}$$

$$\Delta\text{Declination} \approx 0.8 \text{ deg}$$

$$\Delta\text{Uplink (XA)} \approx 17 \text{ Hz (Voltage-controlled oscillator (VCO) level)}$$

These were the same uncertainties assumed for the Helios 1 launch based on estimated 3σ injection condition perturbations. Since new estimates for Helios 2 indicated improved launch vehicle performance, and since Helios 1 and Viking launch pass residuals were orders of magnitude smaller than the above uncertainties, these estimates were considered to be reasonable. However, they were incomplete in the sense that there are "failure modes" of launch vehicle performance which would result in grossly larger errors than those above. Bearing this in mind, the initial acquisition was designed to accommodate possible trajectory uncertainties far in excess of the "nominal" launch vehicle performance induced uncertainties.

C. Prediction Strategy

In order to assure the availability of the best possible predictions in any of the possible launch contingency situations, the following plan for generation of up to eight different predicts sets was adopted:

(1) $L - 7$ days: Approximately seven days before launch three predicts sets would be generated. These sets would be the open, mid and close window cases (designated H15O, H15M, H15C) for the nominal launch date and time. These prelaunch nominal sets would be generated with time from launch (TFL) time and two different sample rates: 20 s/sample until $L + 75$ min and 300 s/sample after that time. (The high angle and frequency rates occur during the first half-hour of the pass.) These sets would be transmitted to DSS 42 and DSS 44 in both text and binary form to serve as backup to the predicts generated on launch day.

(2) $L - 90$ min: At launch minus 90 minutes, a polynomial coefficient tape (PCT) based on the latest launch time would be generated. This PCT combined with the latest available spacecraft frequencies would then be input to the predict run (set H15U) from which the (nominally) prime drive tape would be punched. These predicts would serve in the tracking Real-Time Monitor (RTM) for pseudoresidual calculations as well as for reference as frequency predictions. With a GMT time field, they would have the same sample rates as the $L - 7$ days predicts and reflect the tuning pattern to be used in the uplink acquisition.

(3) $L - 10$ min: In case of a hold during the countdown, generation of a PCT based on the latest estimate of the launch time would commence at about launch minus 10 minutes. The predicts (H15E) generated from this tape and incorporating the latest frequencies would be identical in format to the $L - 90$ min set.

(4) $L + 5$ min: By about launch plus 5 minutes, generation of a PCT based on the actual liftoff time would begin. The "actual launch time" predicts (H15A) produced from this PCT would be identical in format to the "U" and "E" predicts above.

(5) $L + ?$ min: If the solar orbit injection burn did not occur, generation of a parking orbit PCT would start at an appropriate time to allow tracking by the first DSS that would come into view. (There would be a long time span before the spacecraft would come into view of a DSS should it remain in the parking orbit.) The corresponding predicts would be in GMT at a nominal sample rate of 10 s/sample. The set designation would be H15N.

(6) $L + 180$ min: Approximately three hours after launch a PCT based on the Real-Time Computer System (RTCS) estimate of the solar orbit injection state vector would be produced. Predicts from this PCT would have GMT time and a sample rate of 300 s/sample. This set, designated H15I, would extend to approximately launch plus 14 hours.

(7) $L + 9$ h: By launch plus 9 hours the spacecraft is, for most tracking purposes, in "cruise phase." The set of predicts generated at this time would therefore be in a more or less standard multistation format (but extend to only about $L + 30$ hours). Input would be a PCT based on the first orbit solution using S-band radio metric data from DSS 42.

In addition to the JPL predicts, Air Force Eastern Test Range (AFETR) predicts would be generated by the Real-Time Computer System (RTCS), using JPL frequency inputs and ETR trajectory data with three sets to be transmitted during the launch period: a preflight nominal set at launch minus 45 min, a set based on Vanguard C-band data at about launch plus an hour, and a set at launch plus 190 min based on S-band data from DSS 42.

For a nominal or near-nominal launch trajectory, JPL predicts would be prime for all uses and ETR predicts prime only in case of a non-nominal trajectory or when use of JPL predicts was precluded by hardware or software failures.

D. Angle Drive Strategy

The relevant considerations in formulating the angle drive strategy at DSS 42 for the Helios 2 launch phase were the following:

(1) In the silent spacecraft mode, the antenna must be

driven in the blind for a period long enough to acquire an uplink and subsequently to command the spacecraft on.

(2) The low signal strength and signal-to-noise ratio (SNR) characteristic of the interference zone makes it improbable that autotrack can be maintained through the first ~8 minutes of the track (i.e., through the end of the interference zone). If autotrack is broken, the ground antenna begins to drive away from the spacecraft, risking the loss of downlink lock.

(3) Under strong signal conditions, the preferred tracking mode is autotrack.

(4) The uplink should be acquired as quickly as possible after the end of the interference zone (at about rise + 8 m).

(5) The antenna must be on Antenna Pointing Subsystem (APS) drive tape during the switch to two-way coherent (in autotrack the antenna could drive off point when the noncoherent–coherent link switch causes the receivers to drop lock).

Consistent with the above requirements, the basic angle drive strategy was defined:

(1) Computer drive from the best available predicts until downlink lock is established (the spacecraft may be silent) but in any case through the end of the interference zone; then,

(2) As soon as criterion 1 allows, switch to autotrack.

(3) Return to computer drive for the noncoherent–coherent downlink transition, then back to autotrack.

Where this basic strategy called for computer drive, the choice of an appropriate drive tape would be according to the following procedure:

If a verified GMT drive tape based on a launch time that is accurate to ±5 seconds is available, it is used. A time bias correction is applied if the launch time error is greater than 1 second. (The corresponding predict set might be any of the following, depending on the circumstances: H15U, H15A, H15E.) If none of the available (verified) drive tapes satisfies the launch time accuracy criterion, the plan calls for use of a verified H15A or H15E drive tape with a time bias applied so as to correct the launch time to within a second of actual launch time.

Either of these situations would allow use of a drive tape with (at most) a small time bias (a few seconds perhaps). If, however, no GMT tape were available with the desired launch time accuracy and neither the "A" nor "E" drive tape had been punched and verified, it would be necessary to use a preflight nominal verified drive tape in TFL format (H15O, H15M, H15C). The time offset used in this case would be the actual launch time in GMT, a somewhat more risky procedure.

In general, use of a prelaunch nominal drive tape would also require angle offsets. These would be computed from H15E or H15A *page print* predicts, if available; otherwise the Tracking Network Operations Analyst (NOA) would provide angle biases based on the known variation of launch trajectory characteristics with launch time.

The above launch time accuracy criterion may seem overly stringent, but consider that a 5-second error translates to about 1600 Hz error in one-way doppler frequency (D1) and an angular error (0.93 deg) of almost 5 times the offset beamwidth of the S-band cassegrain monopulse (SCM) antenna!

If it should be necessary to use AFETR predicts, it would not be possible to perform the highly automated and optimized initial acquisition strategy that is possible with JPL predictions. The initial acquisition strategy in the event of prime AFETR predicts would be similar to those in the era previous to Pioneer 10, Pioneer 11, Mariner Venus Mercury, Helios 1, and the Vikings. In this case the antenna would be manually driven to the AFETR predictions until it was possible to autotrack on the S-band acquisition antenna (SAA), i.e., at least through the end of the interference zone.

E. One-Way Downlink Acquisition

The one-way downlink acquisition would be relatively less complicated than the uplink and coherent downlink acquisitions, and in the past the DSSs have very rapidly and routinely locked the one-way downlink according to standard procedures; hence, no special procedures were required. However, the following estimates of downlink prediction uncertainty were provided (at S-band):

$$3\sigma \text{ D1 TFREQ} \approx 2500 \text{ Hz}$$

$$3\sigma \text{ D1 Trajectory} \approx 850 \text{ Hz}$$

In addition, it was recognized, an uncertainty in D1 would be introduced by the possibility that actual launch time could differ from the expected time (for which predicts are generated) by up to 5 seconds (see Section II-D on angle drive strategy). This could affect the D1 value by up to 1650 Hz. In the worst case this would be added to the 3σ uncertainties to give a D1 total uncertainty $\approx$ 4300 Hz.

F. Uplink Acquisition Strategy

The impact of the possible silent spacecraft mode and the antenna interference zone on the uplink acquisition strategy was considered in the decision to wait until the end of the interference zone before attempting the uplink acquisition. Otherwise, the plan called for an uplink acquisition that would be quite routine, particularly since the 3σ frequency uncertainties were small. The uncertainties assumed were (at VCO level):

$$\Delta\text{Uplink (trajectory)} \approx 17 \text{ Hz}$$

$$\Delta\text{Uplink (best lock)} \approx 12 \text{ Hz}$$

$$\Delta\text{Uplink (temperature)} = \Delta T \cdot \frac{\partial}{\partial T} \text{(Uplink)} \approx 10 \text{ Hz}$$

To allow for an error of up to 5 seconds in predicted launch time, another 4 Hz was added to the root-sum-square of the probabilistic uncertainties, giving:

$$\text{Total uplink uncertainty} \approx 27 \text{ Hz}$$

These frequency uncertainties were relatively small, and tended to counterbalance the difficulties posed by the possible silent spacecraft mode and the antenna interference zone.

To be extremely conservative (and hence accommodate some of the "non-nominal" launch vehicle performance modes alluded to previously) the above 3σ XA[1] uncertainty was generously padded, resulting in an uplink acquisition search of approximately XA ± 100 Hz.

For this acquisition, a sweep rate of +3 Hz/s was selected because:

(1) A rate of +3 Hz/s would result in an effective rate at the spacecraft of about +150 Hz/s (S-band), which is reasonably close to the geometric mean of the upper and lower sweep limits (200 Hz/s).

(2) It was felt that 3 Hz/s would be close to the limit at which the site could no longer accurately tune the exciter (a manual operation).

Finally, the uplink acquisition would consist of a single uplink frequency sweep in the direction of XA change, placing the ending tracking synthesizer frequency (TSF) near the XA frequency to satisfy a command capability requirement that the difference between TSF and XA be no greater than 110 Hz at VCO level. No additional tuning would be required.

If the first sweep were not successful, a second, contingency sweep was planned. This sweep would be at the same rate as the prime sweep, but would cover a region approximately 50 percent greater (XA ± 150 Hz). It would start about 3½ min after the end of the first sweep, and include a downleg, an upleg, and then a downleg back to TSF.

G. Possible Misacquisitions

The misacquisitions considered were of two kinds: acquisition of a spurious signal in the spacecraft transmitter power spectrum or acquisition of the main carrier on a *ground antenna* sidelobe.

The acquisition plan included a table of possible spurious signals, all about 30 dB below the power level of the main carrier and at various frequency offsets from about 3.5 to 26.5 kHz from the carrier. "The necessary steps to be taken to insure that the locking to a spurious signal, should it occur, be quickly identified and remedied" were specified as follows:

Detection of Spurious Signals

(1) The NOCT and station personnel will be familiar with the possibility of occurrence of a spurious signal lockup and, specifically, with the frequency offsets at which this can occur.

(2) The NOCT (primarily the telemetry and monitor NOAs) will observe and interpret actual vs predicted signal strength.

(3) The NOCT (primarily the track NOA) will observe and interpret pseudoresidual output.

Corrective Action

Break receiver lock on spurious signal and reacquire on carrier.

Concerning the second kind of misacquisition the plan stated: "The possibility exists of locking on a (ground)

[1] "XA" denotes the VCO-level frequency at which the DSS must transmit in order that the doppler-modified S-band uplink at the spacecraft will equal the spacecraft receiver's best-lock frequency.

antenna sidelobe while in autotrack. The following information concerning antenna sidelobes is available:

Angular offset	Loss, dB
N/A (SAA)	−36
0.50 deg (SCM)	−20
1.20 deg (SCM)	−27
1.80 deg (SCM)	−37

If it is suspected (from the above data) that antenna sidelobe lock has occurred, autotrack should be broken and the antenna manually driven to antenna main-beam lock."

All of the foregoing plans and procedures applied to DSS 42 as the prime initial acquisition station. For DSS 44 as backup station the same strategies applied with the following exceptions:

> The uplink acquisition would be performed at DSS 44 only if there should be a failure that would preclude performing the acquisition from DSS 42. Since the acquisition aid antenna at DSS 44 is receive only, the SCM must be used for the uplink acquisition. The narrow halfpower offset of the SCM (0.18 deg) requires very accurate pointing for successful acquisition of the uplink. Thus, it was considered advantageous to go to autotrack on the SCM prior to turning on the transmitter. Finally, because of the higher gain of the SCM and in order to use a familiar power of 1 kW, the uplink acquisition might have to be delayed for several minutes after spacecraft rise so as not to exceed the uplink signal level constraint of −70 dBm.

III. Analysis of Launch Phase Operations

A. Predicts Generation

A basic *sine qua non* for a successful initial acquisition is the availability of tracking predictions incorporating the most current possible knowledge of the spacecraft's trajectory and frequency characteristics. Accordingly, much of the activity of DSS, NOCT and supporting advisory personnel prior to spacecraft rise centers on the generation, validation, transmission and revalidation of various predicts sets.

The first set of predictions generated during the Helios-2 launch countdown was the set designated H15U. The generation process began with delivery by the Helios navigation team of a polynomial coefficient tape (PCT) describing the nominal spacecraft trajectory as viewed at the Australian tracking complex. Frequencies were unchanged from the nominal values supplied earlier by project telecommunications analysts. Transmission of the predicts in both text and binary form and punching and verification of the prime antenna drive tape also proceeded smoothly. The whole process was complete by 04:28:00 GMT, just over an hour before launch.

The launch minus 35 minutes update of spacecraft frequencies showed a change of about 20 Hz in the transmitter reference frequency. This prompted a decision to run the predict set H15E (provided for in acquisition plans in case of a slip in the launch time) even if the launch should occur on time. The new frequency information would be used in this set. When the launch did in fact occur on time (at 05:34:00.8 or 0.8 sec late, actually) this procedure was implemented and the predict set H15E was declared prime for frequency information. Set H15U naturally remained prime for antenna drive. The fact that launch occurred within a second of open window alleviated the need for the set H15A, which was therefore cancelled.

B. Summary of Operations at DSS 42

1. **One-way downlink acquisition.** No information was received from the down-range AFETR stations that the Helios 2 spacecraft was in the silent mode, and in fact, this was apparent when, within seconds of the predicted spacecraft rise time, DSS 42 routinely acquired a one-way downlink. (Obviously, this condition vastly reduced the uncertainties heretofore inherent to the initial acquisition procedure at DSS 42.) Signal levels, however, were about 30 dB lower than expected and the station concluded that they were on an antenna sidelobe. Antenna pointing, on drive tape control because of the interference zone, was manually adjusted and offsets were entered, bringing the signal level to a near-nominal value. The station reported that they were "on the main beam now." With this assurance and once safely out of the interference zone, DSS 42 switched antenna drive to autotrack for the brief period of noncoherent tracking to follow.

2. **Interference zone.** The effect of the interference zone on signal levels was minor. The degradation of about 8 or 9 dB that did occur (as seen in the SAA receiver) was completely masked in the SCM receiver by losses due to pointing error (since the SCM antenna has a very narrow beamwidth). Neither receiver lost lock during the interference zone although spin modulation effects resulted in a very high doppler noise level.

3. **Uplink acquisition.** Uplink tuning began on schedule while, coincidentally, antenna pointing was being manually adjusted. Despite the fact that the pointing adjustment involved some rather large antenna excursions (up to 0.8 deg from nominal), pointing errors had no impact on the uplink acquisition since uplink transmission was through the broadbeam SAA antenna. Telemetry data confirmed that nominal uplink acquisition had occurred when the spacecraft receiver's automatic gain control reading dropped precipitously in response to DSS 42's powerful S-band signal.

4. **Two-way noncoherent tracking.** The brief period (about 12 min) of two-way noncoherent tracking following the uplink acquisition proceeded routinely up to the time of the command that would cause the spacecraft to shift its downlink signal to coherent with the uplink. In preparation for this command and the resulting receiver-out-of-lock condition, DSS 42 returned antenna drive to computer mode (drive tape) with offsets to compensate for the angle biases observed during the autotrack period.

5. **Reacquisition of (coherent) downlink.** After dropping lock due to the coherent command, receivers were in lock again only 20 seconds later, but at a signal level some 30 dB below the predicted value. The low signal level evoked some discussion among Network Operations Control Team (NOCT) and advisory personnel and between DSS 42 and the tracking controller at JPL as to whether a sideband (i.e., a spurious signal) acquisition or a sidelobe acquisition had occurred. Finally, after locking up and retuning receivers twice and after performing manual adjustments to antenna pointing angles, DSS 42 obtained solid receiver lock on the spacecraft's carrier signal, at normal levels. The period from first receiver-out-of-lock condition (due to switch in downlink frequency) until receiver lockup on the coherent downlink carrier was about 6 min 15 s. Quantitative details of the reacquisition may be seen in the graph of hour angle residuals and doppler residuals in Figs. 3 and 4, respectively.

The remainder of the DSS 42 pass, for most tracking purposes a routine cruise-phase operation, proceeded smoothly and without incident.

C. Summary of Operations at DSS 44

The one-way downlink signal was acquired less than 20 s after the predicted rise time. (Network Control System Block II Real Time Monitor data show receiver lock was sustained from 06:24:15 GMT. The station reported (presumably intermittent) lock as early as 06:23:52.) Two-way coherent downlink was acquired on the main carrier just 17 s after loss of lock occurred as a result of the spacecraft's switch to a coherent downlink. (Receiver out-of-lock (ROL) was at 06:46:43 and receiver in-lock (RIL) was at 06:47:10.) In another 20 seconds, data from DSS 44 was being correctly flagged as three-way. Autotracking was resumed and the pass continued to spacecraft set without event.

One anomaly during the pass was quickly noticed and corrected by alert DSS 44 personnel. Moments after spacecraft rise and a flawless acquisition of the downlink, the station reported a problem with the X-angle antenna drive. The erratic behavior of the drive can be clearly seen in the graph of the pseudoresidual for the X-angle shown in Fig. 5. The dramatic effect of the station's corrective action—manual peaking of the signal and subsequent switchover to autotrack—is equally clear in the plot of signal level from the SCM antenna (Fig. 5).

It is worthy of note that the forced switch to autotrack occurred before the interference zone and hence DSS 44 tracked throughout the zone in autotrack mode with no harmful results!

D. Prediction Accuracy

It is always of interest to compare the preflight estimates of uncertainties in tracking observables with the pseudoresiduals that result from differencing predicts and actual radio metric data.

In the case of the angle residual, the first point of interest occurred only after antenna drive was switched to autotrack at 06:33:30. After a brief transient in antenna drive response the hour angle residual was 0.30 degrees. Since the preflight uncertainty estimates are estimates of the *maximum* 3σ deviations from nominal (which typically occur at spacecraft rise), it is necessary to extrapolate the angle residuals back to the rise time in order to make a meaningful comparison. From Fig. 3, which presents a profile of the hour angle residual for the first half-hour, a rough graphical extrapolation yields for the hour angle residual at rise (i.e., at $\sim$06:24):

$$\Delta \text{HA} \approx 0.95 \text{ deg}$$

(The first two points occur during the antenna drive transient mentioned above and should not be used in the extrapolation.) Of this total "error," about 0.13 deg is accounted for by the fact that the actual launch time was 0.8 s later than the nominal time, on which tracking predicts were based. Making a liberal allowance of 0.05 deg for possible antenna misalignment leaves 0.77 deg as an indicated trajectory-dependent error. Based on the assumed 3σ hour angle uncertainty of 1.2 deg from Section II, a statistical table assigns a probability of only 5 percent to the class of errors of this size or larger. Thus if the trajectory uncertainty estimates are realistic, the Helios-2 trajectory was a one-in-twenty case. (The somewhat remote possibility that antenna pointing inaccuracies exceeded the 0.05 deg quoted above will be routinely pursued.)

By contrast to the hour angle residual, the declination angle residual held close to an average of

$$\Delta \text{DEC} \approx 0.11 \text{ deg}$$

a value that is in no way remarkable: statistically speaking, about 2 out of 3 cases can be expected to have a trajectory-dependent declination angle residual of this magnitude or greater.

The one-way doppler residual represents an intermediate case. The probability associated with the peak value of

$$\Delta \text{D1} \approx (-)\, 783 \text{ Hz}$$

at rise is about 25 percent after adjusting for the launch time discrepancy of 0.8 s. Here it is impossible to separate the distinct components of the residual which arises in part from uncertain knowledge of the spacecraft's auxiliary oscillator frequency (which provides a reference for generation of the noncoherent downlink frequency) and in part from uncertain knowledge of the spacecraft's radial velocity (which determines the amount of doppler shift on the downlink).

E. Uplink Acquisition at DSS 42

Based on guidelines as summarized in Section II, the instructed uplink acquisition sweep was defined as:

Ramp start time	06:31:00 GMT
Starting frequency	22.017880 MHz (VCO)
Frequency rate	3 Hz/s (VCO)
Ramp end time	06:32:20 GMT
Ending frequency	22.018120 MHz (VCO)
Sweep duration	80 s

The instructed sweep and the sweep actually executed by DSS 42 can be seen in Fig. 6. The station tuned manually at a remarkably constant rate of about 2.5 Hz/s or about 85 percent of the instructed rate. Due to a late start (about 10 s late) and the slow tuning rate, the final tracking synthesizer frequency (TSF) was achieved some 25 s late. These minor departures from the nominal sweep parameters had no effect on the success of the acquisition.

F. Comments on the Interference Zone

A number of observations on the interference zone, theory and practice, are in order. First, this author's own Initial Acquisition Plan implies that the principal feature of the interference zone is low signal levels. This is inaccurate. The "low signal level" feature per se is insignificant—just an hour after the zone, the spacecraft's signal level is lower than the minimum value reached during the zone, this being due merely to space loss. (Ground receiver automatic gain control (AGC) data show a maximum interference zone degradation of about 10 dB.) The interference zone is characterized, theoretically at least, by a rapidly changing signal level or, in effect, amplitude modulation. This could (in theory) make autotracking marginal or impossible; in point of fact, however, DSS 44 autotracked through the entire zone without difficulty!

The most noticeable effect on tracking data shows in the extreme degree of corruption to doppler data that results from the very heavy spin (frequency) modulation of the spacecraft's downlink. This assumes that receiver lock is maintained throughout the period of severest modulation, as was indeed the case with receivers at both DSS 42 and DSS 44.

G. The Effects of Spin Modulation on Doppler Data

Although experience in two Helios initial acquisitions has shown that the spin modulation effects of the offset low-gain antenna are not severe enough to disrupt a carefully planned acquisition procedure, it would be helpful to be able to predict the effects of spin modulation on observable tracking quantities. If the maximum effects are known in advance, it is possible to identify at least any anomaly that is not masked by spin modulation effects and to take appropriate steps to determine the source of such an anomaly.

It is in fact quite easy to derive a theoretical expression for the maximum effect of spin modulation on doppler data. A simplified derivation of the effect is presented below, on the assumption that what is measured by the DSS doppler system is the real doppler shift of the spacecraft's downlink frequency. A more complete derivation yields the same result up to an (uninteresting) additive constant in the indicated one-way doppler frequency.

Let $\boldsymbol{\omega}$ denote the spacecraft's spin vector in rad/s, and let $\hat{L}$ be a unit vector along the line of sight from the spacecraft to DSS 42. Now define an orthogonal coordinate system as follows: let $\hat{l}$ denote the unit vector perpendicular to $\boldsymbol{\omega}$ that lies in the plane of $\boldsymbol{\omega}$ and $\hat{L}$. Let $\hat{n} = \boldsymbol{\omega}/|\boldsymbol{\omega}|$ and choose the unit vector $\hat{m}$ to complete the right-handed orthogonal system $\hat{l}$, $\hat{m}$, $\hat{n}$ (Fig. 7). Now since the velocity vector $\mathbf{v}_s$ of the horn antenna is orthogonal to $\boldsymbol{\omega}$ it has no n component. Furthermore, we have chosen our coordinate system so that $\hat{L}$ has no m component. Consequently the component of antenna velocity along the line-of-sight, $\mathbf{v}_s \cdot \hat{L}$, is just the product of the l components of $\mathbf{v}_s$ and $\hat{L}$ (the products of the m and n components each involve a factor zero):

$$\mathbf{v}_s \cdot \hat{L} = v_{s_l} L_l + v_{s_m} \cdot 0 + 0 \cdot L_n$$

or

$$\mathbf{v}_s \cdot \hat{L} = v_{s_l} L_l \tag{1}$$

Now $\mathbf{v}_s$ is just the velocity vector of a point in uniform circular motion in the lm plane so its l component varies sinusoidally. We may then write

$$v_{s_l} = v_s \cos \omega t = 6\lambda\omega \cos \omega t \tag{2}$$

where λ is the wavelength of the spacecraft's S-band downlink signal and 6λ is the distance of the horn antenna from the spin axis (a convenient relationship designed into the spacecraft).

Now if θ is the angle between $\hat{L}$ (line-of-sight vector) and $\hat{n}$ (or $\boldsymbol{\omega}$), the l component of $\hat{L}$ is just (recall that $\hat{L}$ is in the ln plane):

$$L_l = \sin \theta$$

Putting this result and Eq. (2) into (1), we have

$$\mathbf{v}_s \cdot \hat{L} = v_{s_l} L_l = 6\lambda\omega \sin \theta \cos \omega t \tag{3}$$

for the component of the antenna's spin velocity along the line-of-sight to the ground station. We will call this the radial spin velocity component:

$$\dot{r}_s = \mathbf{v}_s \cdot \hat{L} = 6\lambda\omega \sin \theta \cos \omega t \tag{4}$$

Now, defining the following additional symbols:

c = speed of light *in vacuo*

$f_{s/c}$ = spacecraft's S-band downlink frequency (Hz)

f_{dop} = change of downlink frequency due to the doppler effect

$\dot{r}$ = antenna's total line-of-sight (radial) velocity

$\dot{r}_{cm}$ = radial velocity of spacecraft center of mass

Δt = doppler sampling interval

we can write (noting that $\lambda = c/f_{s/c}$):

$$f_{dop} = f_{s/c} \frac{\dot{r}}{c} = \frac{\dot{r}}{\lambda} = \frac{1}{\lambda}(\dot{r}_{cm} + \dot{r}_s)$$

$$= \frac{\dot{r}_{cm}}{\lambda} + \frac{1}{\lambda}(6\lambda\omega \sin \theta \cos \omega t)$$

where we have used the expression (4) for $\dot{r}_s$. Thus

$$f_{dop} = \frac{\dot{r}_{cm}}{\lambda} + 6\omega \sin \theta \cos \omega t \tag{5}$$

The first term $\dot{r}_{cm}/\lambda$ represents the usual doppler shift of a nonrotating spacecraft while the term $6\omega \sin \theta \cos \omega t$ is the spin modulation term that is superimposed when the spacecraft is rotating. (The time derivative of the second term gives the instantaneous rate of change of the downlink frequency due to the spacecraft rotation:

$$\dot{f}_s = -6\omega^2 \sin \theta \sin \omega t$$

This formula was used to estimate the receiver stress that could be expected due to the high rate of change of the spacecraft's signal in Section II-B.)

Now the instantaneous doppler frequency is not directly observable in the DSS instrumentation. What is displayed in near-real-time, and recorded for later analysis, is the difference (called a pseudoresidual) between an average doppler frequency, periodically determined at intervals Δt, and the predicted doppler frequency for the corresponding time. The average frequency is measured by continuously counting doppler cycles (extracted from the downlink signal by a method that need not concern us here), differencing successive sampled counts C_i and dividing by the time interval Δt between samples: symbolically

$$\Delta C_i = C_{i+1} - C_i$$

and

$$\bar{f}_{dop} = \frac{\Delta C_i}{\Delta t}$$

Then clearly

$$\begin{aligned}\Delta C &= \int_t^{t+\Delta t} f_{dop}\, dt \\ &= \int_t^{t+\Delta t} \frac{\dot{r}_{cm}}{\lambda}\, dt + \int_t^{t+\Delta t} (6\omega \sin\theta \cos\omega t)\, dt \\ &= \frac{\Delta r_{cm}}{\lambda} + 6\omega \sin\theta \int_{\omega t}^{\omega(t+\Delta t)} \cos\phi \frac{d\phi}{\omega} \\ &= \frac{\Delta r_{cm}}{\lambda} + 6 \sin\theta \text{ "}\Delta \sin\phi\text{"}\end{aligned}$$

where $\phi = \omega t$ and

$$\begin{aligned}\text{"}\Delta \sin\phi\text{"} &= \sin(\omega t + \omega \Delta t) - \sin\omega t \\ &= \sin(\phi + \Delta\phi) - \sin\phi\end{aligned}$$

(Note that we have used the fact that θ is slowly varying to bring $\sin\theta$ out of the integrand: over the sample intervals of interest (1 sec to 10 sec) the spacecraft DSS line-of-sight may be considered fixed, hence θ is constant.)

Now we can write an expression for the computed estimate of the doppler frequency:

$$\bar{f}_{dop} = \frac{\Delta C}{\Delta t} = \frac{1}{\lambda}\frac{\Delta r_{cm}}{\Delta t} + \frac{6\sin\theta}{\Delta t}\text{"}\Delta \sin\phi\text{"} \quad (6)$$

Since the "center-of-mass" doppler shift $(1/\lambda)(\Delta r_{cm}/\Delta t)$ can be predicted to a high degree of accuracy, the pseudoresidual (measured doppler less predicted center-of-mass doppler) may be written as

$$\text{Doppler residual} = \frac{6\sin\theta}{\Delta t} \text{"}\Delta \sin\phi\text{"} + \text{linear bias term} \quad (7)$$

for small sample intervals. The "linear bias term" can be easily removed by a linear regression over a number of successive samples. Such a "detrending" of the doppler residual is in fact performed by the Real Time Monitor (RTM) so that the term

$$\bar{f}_s \equiv \frac{6\sin\theta}{\Delta t} \text{"}\Delta \sin\phi\text{"} \quad (8)$$

may be observed directly in near-real-time.

The first thing we may say about this spin modulation residual is that the maximum possible value for a given θ is

$$\frac{12\sin\theta}{\Delta t}$$

since the factor "$\Delta \sin\phi$" can be at most 2. Let us write out the term in full:

$$\begin{aligned}\text{"}\Delta \sin\phi\text{"} &= \sin(\phi + \Delta\phi) - \sin\phi \\ &= \sin(\omega t + \Delta\phi) - \sin\omega t\end{aligned}$$

We have written $\Delta\phi$ instead of $\omega\Delta t$ to emphasize that $\Delta\phi$ is a constant (for given sample interval Δt). The actual maximum depends on the instantaneous value of $\phi = \omega t$ at the sample time. Thus we wish to determine

$$\max_{\phi} [\sin(\phi + \Delta\phi) - \sin\phi].$$

The value ϕ_0 of ϕ that gives this maximum value may be determined by equating the derivative of "$\Delta \sin\phi$" with respect to ϕ to zero and solving for $\phi = \phi_0$. This gives

$$\begin{aligned}\frac{d}{d\phi}\text{"}\Delta \sin\phi\text{"} &= \cos(\phi + \Delta\phi) - \cos\phi \\ &= \cos\phi \cos\Delta\phi - \sin\phi \sin\Delta\phi - \cos\phi \\ &= (\cos\Delta\phi - 1)\cos\phi - \sin\phi \sin\Delta\phi = 0\end{aligned}$$

which implies that

$$\begin{aligned}(\cos\Delta\phi - 1)\cos\phi &= \sin\phi \sin\Delta\phi \\ \tan\phi &= \frac{\cos\Delta\phi - 1}{\sin\Delta\phi} \\ &= \tan(-\Delta\phi/2)\end{aligned}$$

This last line may be obtained by writing $\Delta\phi$ in the preceding line as $2(\Delta\phi/2)$ and applying the double angle formulas for $\cos\Delta\phi$ and $\sin\Delta\phi$.

Then, of course,

$$\phi_0 = -\frac{\Delta\phi}{2}$$

and

$$\begin{aligned}\text{"}\Delta \sin\phi_0\text{"} &= \sin(\phi_0 + \Delta\phi) - \sin\phi_0 \\ &= \sin\frac{\Delta\phi}{2} - \sin\left(-\frac{\Delta\phi}{2}\right) \\ &= 2\sin\frac{\Delta\phi}{2}\end{aligned}$$

This formula actually gives the maximum or minimum value of "$\Delta \sin \phi$" depending on the sign $\Delta\phi$ (minimum if $\Delta\phi < 0$, maximum if $\Delta\phi > 0$) but note that

$$\min(\text{“}\Delta \sin \phi\text{”}) = -\max(\text{“}\Delta \sin \phi\text{”})$$

and we are really interested only in the *magnitude* of "$\Delta \sin \phi$." Hence

$$\max_{\phi} |\bar{f}_s| = \frac{6 \sin \theta}{\Delta t} \max_{\phi} |\text{“}\Delta \sin \phi\text{”}|$$

$$= \frac{6 \sin \theta}{\Delta t}\left(2 \sin \frac{\omega \Delta t}{2}\right) \text{ for one-way doppler} \tag{9}$$

It is easily shown that the spin modulation effect on two-way doppler is just twice the effect on one-way doppler (except for the turnaround ratio, which for our purposes is negligible). Hence

$$\max_{\phi} |\bar{f}_s| = \frac{12 \sin \theta}{\Delta t}\left(2 \sin \frac{\omega \Delta t}{2}\right) \text{ for two-way doppler} \tag{10}$$

Table 1 shows these expressions evaluated for several combinations of ω, Δt and θ that are of interest.

A comparison of the above prediction to reality may be made by consulting Fig. 8. It shows the one-way doppler residuals seen during the Helios 2 launch pass over a brief period just after the uplink tuning. As can be seen, the maximum deviation of the samples from the detrender line is very nearly the value predicted by the above theory, namely 6.3 Hz (see Table 1).

IV. Summary and Conclusions

Tracking operations during the Helios 2 launch phase proceeded smoothly with two exceptions: (1) an antenna drive component failure at DSS 44 necessitated a brief departure from the planned antenna drive scheme, and (2) spurious signal acquisitions slightly delayed the carrier reacquisition after the transition from noncoherent to coherent downlink. Neither of these problems had a serious effect on the DSN's ability to provide good tracking data and reliable telemetry and command links to the spacecraft. On the whole, planning and preparation for the launch were thorough and sound, and as a result the launch phase operations may be judged a solid success.

Acknowledgments

The author is grateful to the following persons for their assistance in the preparation of this report: A. Berman and R. Schlaifer, who checked for technical accuracy and made a number of helpful suggestions; M. Humnicky, R. Brady and G. Hiendlmeier, who provided valuable data; M. Cates and C. Darling who are responsible for the fine graphical illustrations; and F. Almon for her very fast and accurate typing support.

Table 1. Maximum spin modulation effects on doppler

RPM[a]	Δt, s	$\Delta\phi$, deg	θ, deg	Doppler mode	Max $\bar{f}_s$, Hz	GMT[b]
96.00	1	216.0	90	1-way	11.4	–
87.95	1	167.7	90	1-way	11.9	–
87.95	1	167.7	32	1-way	6.3	06:33:00
50.34	10	−58.0	90	2-way	2.2	–
50.34	10	−58.0	10	2-way	0.4	08:00:00

[a]RPM = spacecraft spin rate in revolutions per minute.

[b]GMT (on January 15, 1976) at which the condition actually applied during the Helios 2 launch phase.

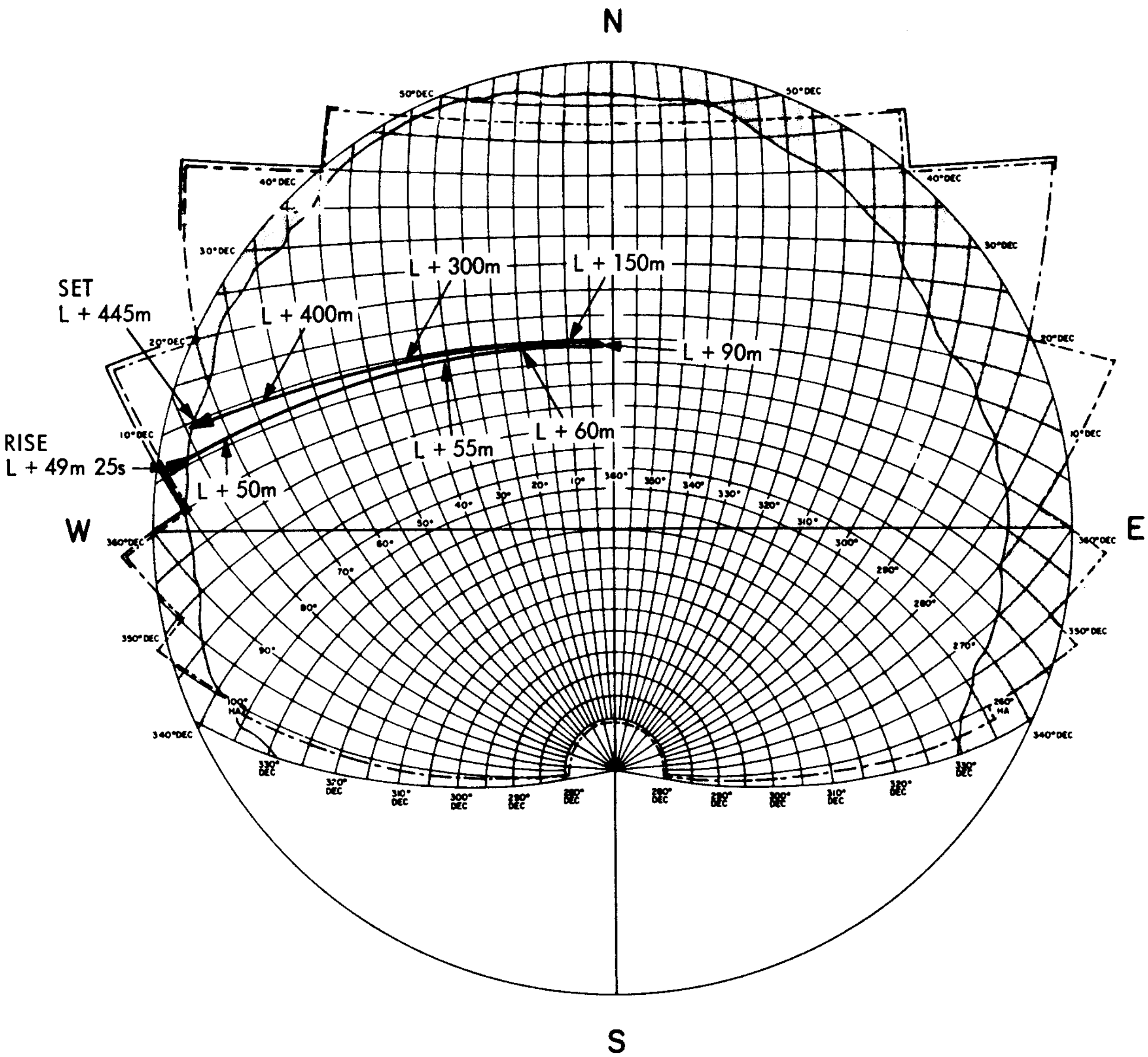

ANTENNA LIMITS					
DEC	PRE	FINAL	HA	PRE	FINAL
DN	047.400	047.992	H1E	305.400	304.886
D2E	039.540	040.404	H2E	285.280	284.850
D3E	019.520	020.432	H3E	275.250	274.788
D4E	359.530	000.320	H4E	265.450	264.840
D5E	349.630	350.376	H5E	260.160	258.876
D6E	336.550	337.440	H6E	257.600	257.264
D2W	39.500	040.374	H1W	054.450	055.175
D3W	019.500	020.414	H2W	074.500	075.314
D4W	359.500	000.314	H3W	084.750	085.290
D5W	349.600	350.370	H4W	094.220	094.918
D6W	336.550	337.434	H5W	099.320	100.262
DS	280.480	279.916	H6W	101.780	102.428

TIDBINBILLA STATION DSIF 42
HA-DEC COORDINATES
STEREOGRAPHIC PROJECTION
REV-I JPL 3109 MARCH 69

Fig. 1. Stereographic projection of Helios-2 launch pass at DSS 42

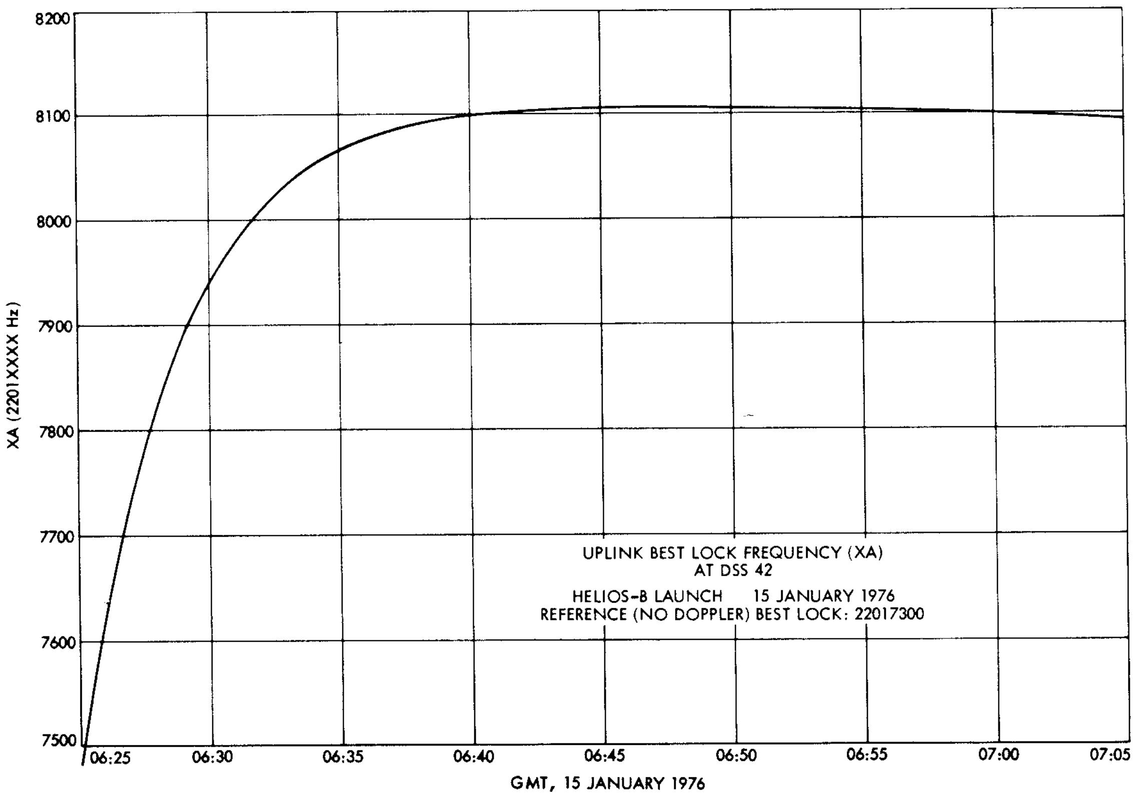

Fig. 2. Uplink best-lock frequency (XA) at DSS 42

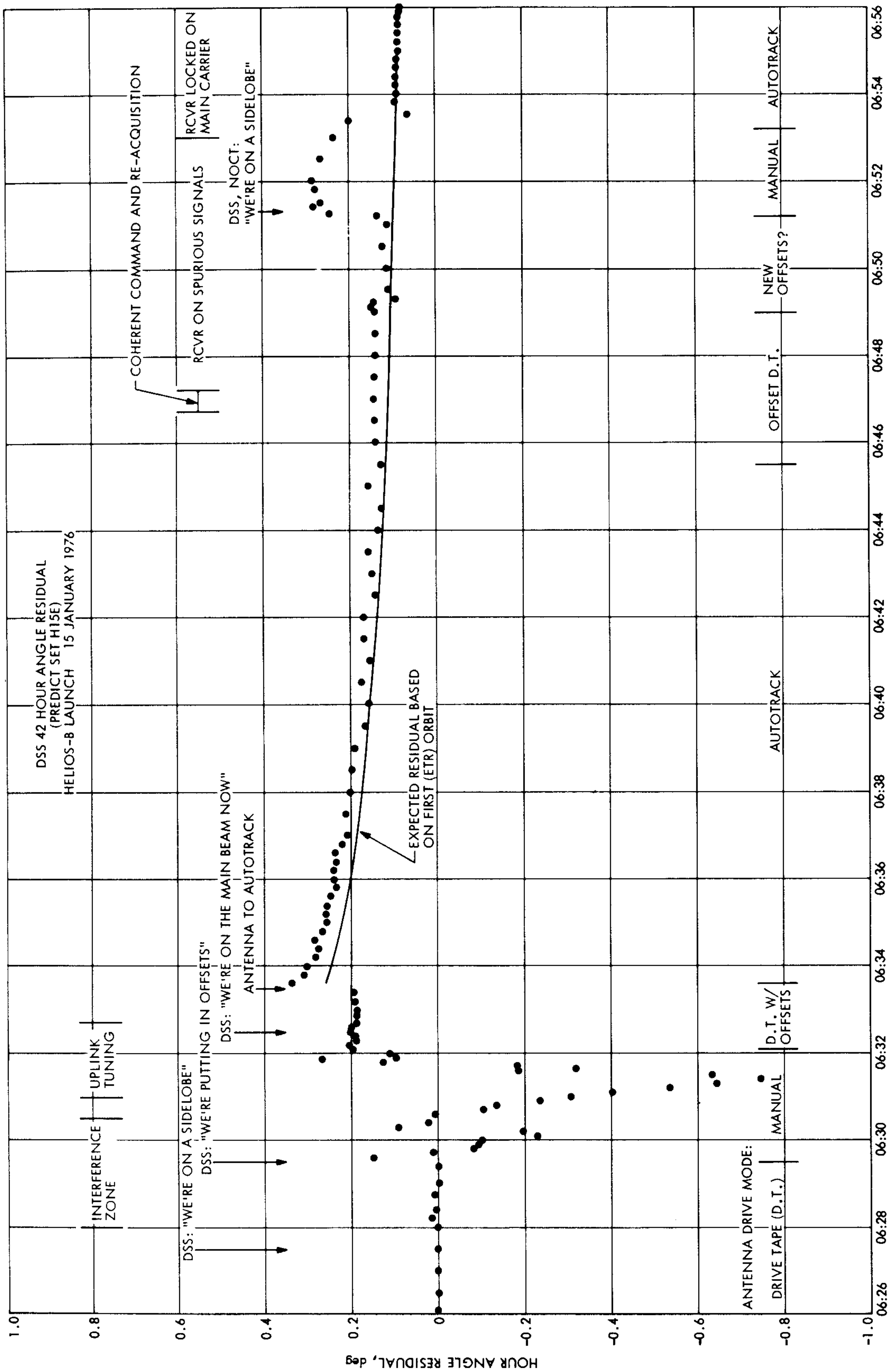

Fig. 3. DSS 42 hour angle residual

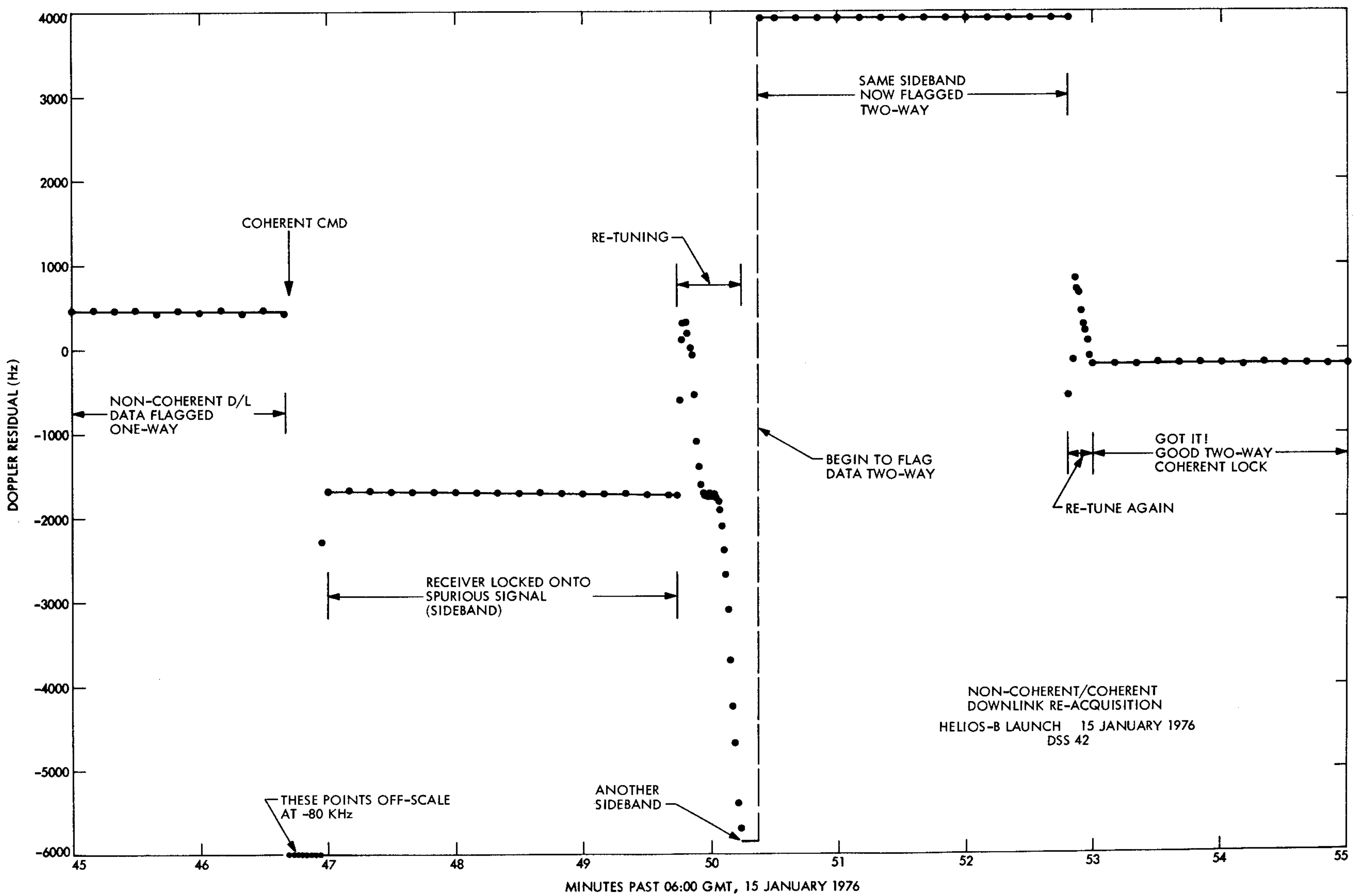

Fig. 4. Noncoherent/coherent downlink reacquisition at DSS 42

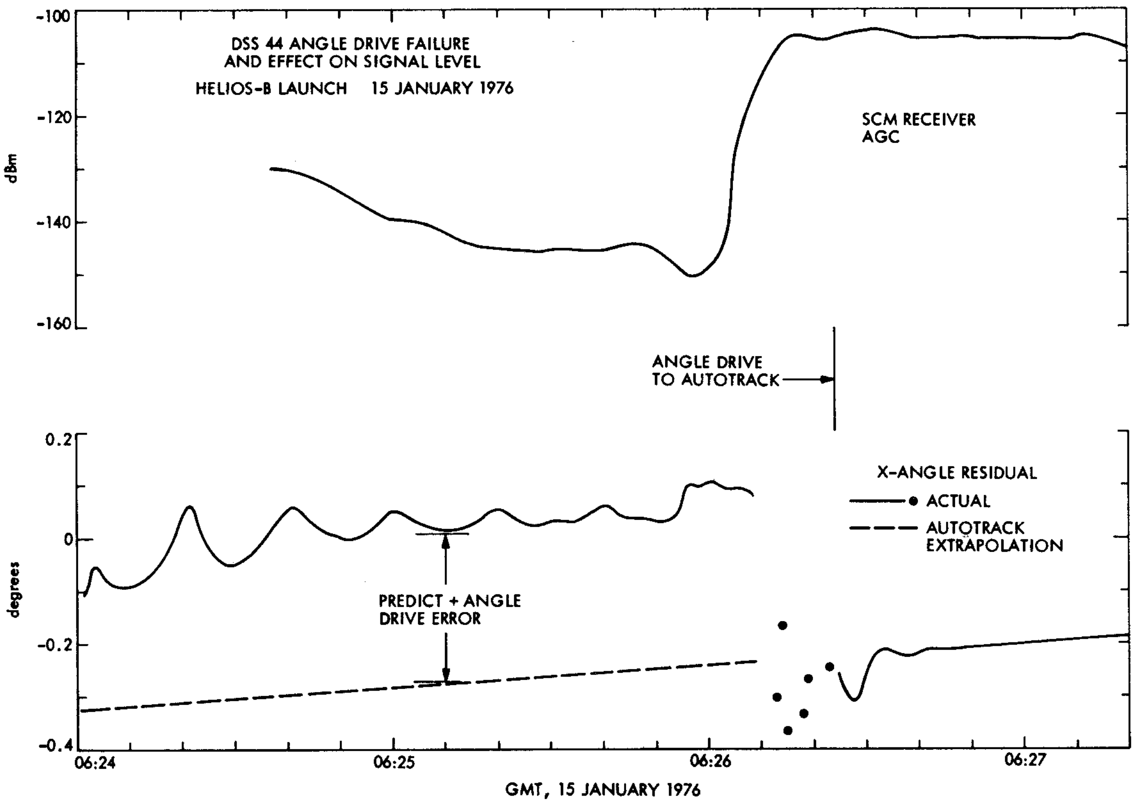

Fig. 5. DSS 44 angle drive failure and effect on signal level

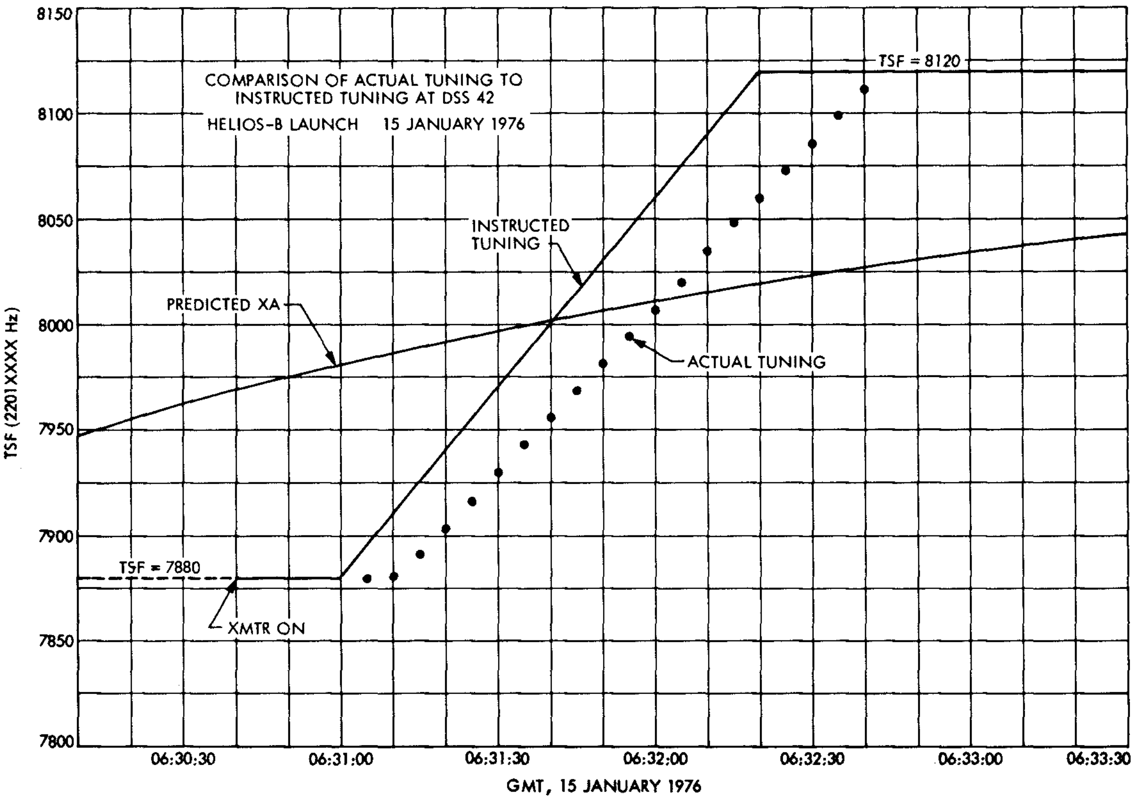

Fig. 6. Comparison of actual tuning to instructed tuning at DSS 42

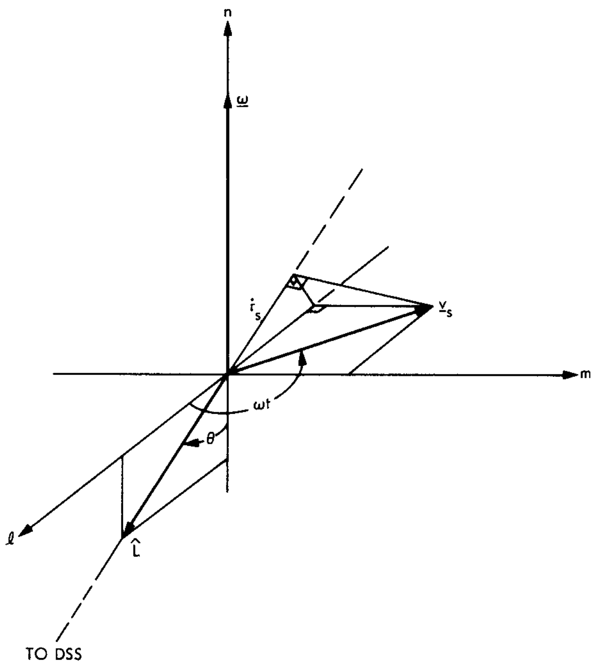

Fig. 7. Spin-modulation geometry

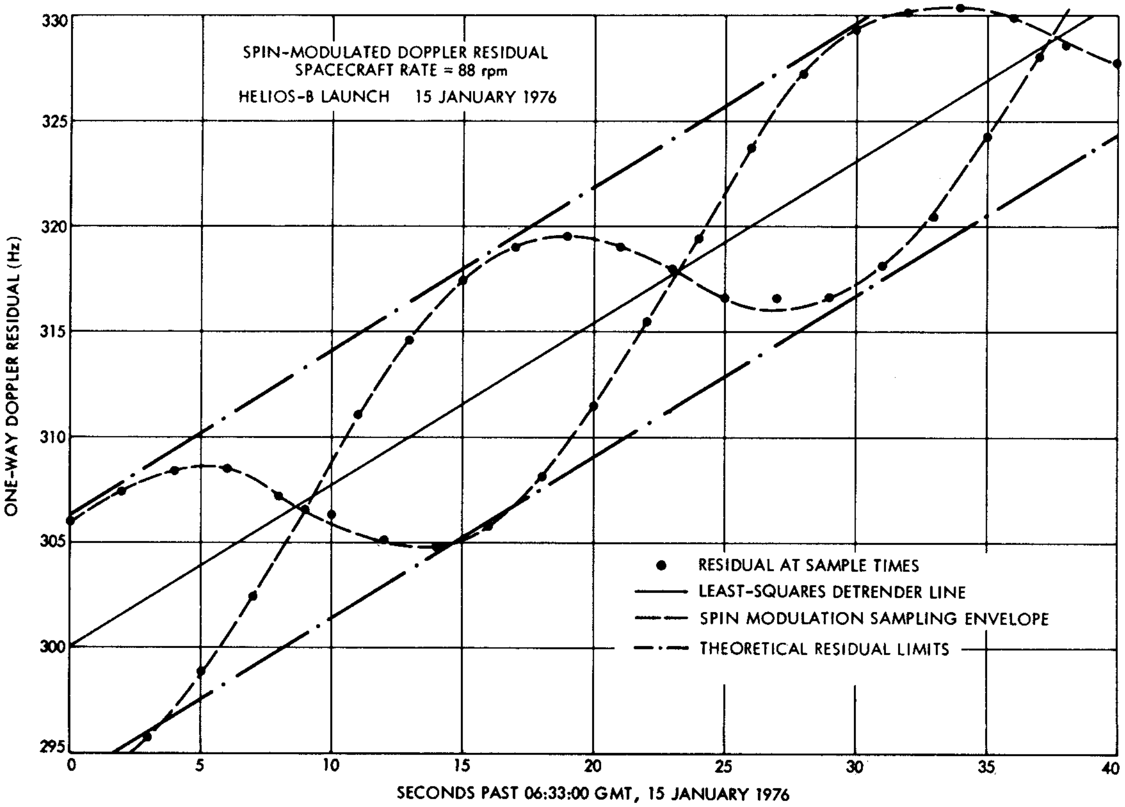

Fig. 8. Spin-modulated doppler residual